

MODELING OF RADAR SCATTERING FROM OIL FILMS

Nicolas Pinel and Christophe Bourlier
IREENA Laboratory – Radar Team
Polytech’Nantes, Université de Nantes
Nantes, France
nicolas.pinel@gmail.com

Abstract— Oil films on the sea surface damp the capillary waves of the surface height spectrum. This hydrodynamic damping influences the normalized radar cross section (NRCS) of contaminated seas, comparatively to clean seas. First, a simple appropriate damping model is presented with parameters that match experimental results. Second, the two-dimensional bistatic NRCS of the contaminated sea surface is presented by comparison with that of a clean sea.

Electromagnetic scattering by rough surfaces, Random media, Sea surface, Water pollution, Multistatic scattering

I. INTRODUCTION

In order to model the power scattered by either clean or contaminated seas (i.e., oil films on the sea surface), a good hydrodynamic modeling of the surfaces is necessary. That is to say, the surface height probability density function (PDF) and the surface height spectrum (equal to the Fourier transform of the surface height autocorrelation function) must be determined. In this paper, the case of insoluble homogeneous oil films on the sea surface is considered, which is valid for wind speeds u_{10} inferior to approximately 8 or 10 m/s. Moreover, the two air/oil and oil/sea interfaces are assumed to be identical and parallel, which can be considered for most cases in oil spill detection.

Next, an appropriate electromagnetic modeling for both clean and contaminated seas can be made. This step can be resolved by using “exact” numerical methods, even though this way demands extensive computing time and memory space for the case of contaminated seas. Such methods can then be used as reference methods in order to validate asymptotic models which will preferably be used for the sake of fastness in computing time. For the case of sea-like surfaces, first works on this subject used a two-scale model [1,2]. More sophisticated asymptotic models can be used, typically, the small slope approximation or the weighted curvature approximation [3].

In [section II](#), the influence of an oil film over a sea surface on the surface height spectrum is studied: the surface height spectrum of a contaminated sea (for both air/oil and oil/sea interfaces), S_{cont} , is presented and compared with the one of a clean sea, S_{clean} , given by the Elfouhaily et al. model [4]. For a contaminated sea surface, the Lombardini et al. model [5] is used for both air/oil and oil/sea interfaces (which are considered to be strictly identical and parallel in the following), which does not explicitly depend on the oil film thickness. Last, with the knowledge of the relative permittivities of the sea and the oil media, the two-dimensional normalized radar cross section (with one-dimensional surfaces) of a contaminated sea is compared in [section III](#) to that of a clean sea.

II. HYDRODYNAMIC MODELING: SURFACE SPECTRUM OF CLEAN AND CONTAMINATED SEAS

In this section, the hydrodynamic modeling of clean and contaminated seas is led, by considering that the two (air/oil and oil/sea) interfaces of the contaminated case obey the same statistics, i.e. have the same surface height PDF and spectrum. For both clean and contaminated seas, the surface height PDF is assumed to be Gaussian. For a clean sea, the surface spectrum is assumed to obey the Elfouhaily et al. model [4]. In what follows, the surface spectrum of a contaminated sea is studied more thoroughly.

Lombardini et al. [5] demonstrated that ripples on a water surface covered by an oil film exhibit a damping effect, which is characterized by a maximum located in the gravity-capillary region of the spectrum, around the frequency $f = 10$ Hz. This damping effect is expressed by an attenuation coefficient γ [5], which is usually called the Marangoni viscous damping coefficient [6,7]. In the Lombardini et al. model, the damping coefficient γ depends on two parameters, namely, the elasticity modulus E_0 , and the characteristic pulsation ω_D . Here, a sea covered by an insoluble oil film is considered (for soluble films, see [1,8] for instance). Then, ω_D depends on the structural relaxation between intermolecular forces. It must be noted that contrary to simulations led by the authors in [5] which consider organic films, we are here in the case of oil films. This implies that the simulation parameters (E_0 and ω_D) to be used can take *a priori* different values than the typical ones in [5]. This was confirmed recently from experiments [14,15], in which it was concluded that the elasticity values E_0 are smaller for oil films than for organic films, and smaller than

10 mN/m [15]. Thus, previous works [5,9], which used parameters more typical of organic films, are not very appropriate parameters of the damping model of oil films.

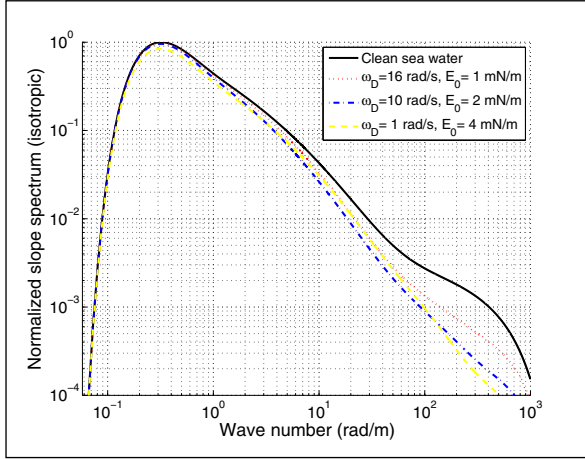


Figure 1. Normalized slope spectrum (isotropic part) of clean and contaminated sea surfaces versus the wave number k . The wind speed is $u_{10} = 6$ m/s.

Experience gained from experimental results [14,15] (more precisely, Fig. 4 of [15] and Fig. 3 of [14]), together with the Cox and Munk experimental results on the surface root mean square (RMS) slopes [16] allowed us to estimate the range of E_0 between approximately 1 and 4 mN/m. Thus, in what follows, three different cases are presented.

In Fig. 1, the normalized slope spectrum (isotropic part) of a contaminated sea surface, $k^2 S_{\text{cont}} = k^2 M(k)/y$, is plotted versus the wave number k for $\{\omega_D = 16 \text{ rad/s}, E_0 = 1 \text{ mN/m}\}$, $\{\omega_D = 10 \text{ rad/s}, E_0 = 2 \text{ mN/m}\}$, and $\{\omega_D = 1 \text{ rad/s}, E_0 = 4 \text{ mN/m}\}$. The wind speed is $u_{10} = 6$ m/s, and the normalization is done by dividing the slope spectrum by the square of RMS slope of the clean sea water $\sigma_s^{\text{clean}} = 0.186$. For comparison, the normalized slope spectrum (isotropic part) of a clean sea surface given by the Elfouhaily et al. model [4], $k^2 S_{\text{clean}} = k^2 M(k)$, is plotted versus the wave number k . As expected, one can observe in Fig. 1 that the oil film strongly damps the high frequencies corresponding to the capillary waves. Comparatively to higher values of E_0 , which typically correspond to organic films, the damping in the high frequencies is in general weaker for oil films than for organic films. Moreover, the damping is stronger for $\{\omega_D = 1 \text{ rad/s}, E_0 = 4 \text{ mN/m}\}$ than for $\{\omega_D = 10 \text{ rad/s}, E_0 = 2 \text{ mN/m}\}$, which is stronger than for $\{\omega_D = 16 \text{ rad/s}, E_0 = 1 \text{ mN/m}\}$. In what follows, the impact of the oil damping on the surface height auto-correlation function and on the surface RMS slope is studied.

III. HEIGHT AUTOCORRELATION FUNCTION AND RMS SLOPE OF CLEAN AND CONTAMINATED SEAS

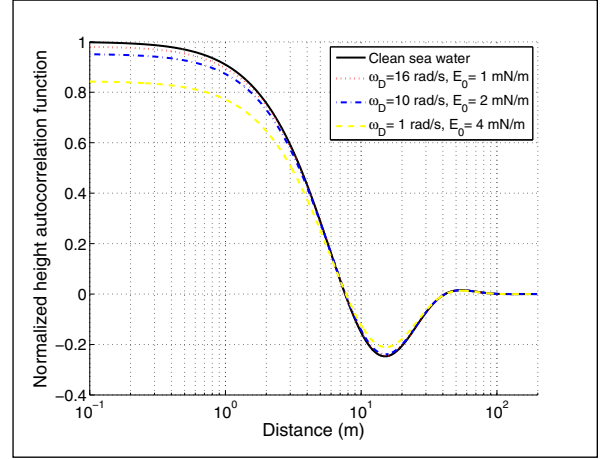


Figure 2. Normalized height autocorrelation function W_0 of clean and contaminated seas versus the distance. The wind speed is $u_{10} = 6$ m/s.

Here, we are interested in the height autocorrelation function W_0 , which is equal to the inverse Fourier transform of the surface height spectrum. For a 1-D surface, using the same parameters as for the height spectrum, the normalized height autocorrelation function is plotted in Fig. 2 for a wind speed $u_{10} = 6$ m/s. That is to say, the three autocorrelation functions are divided by the square of the clean sea water RMS height $\sigma_h^{\text{clean}} = 0.232$ m. It can be seen that because the capillary waves are strongly damped by the oil film, the amplitudes of the height autocorrelation function for the surfaces of the oil film are smaller than those for a clean sea surface for small distances. Moreover, it is smaller for smoother films (i.e., the case $\{\omega_D = 1 \text{ rad/s}, E_0 = 4 \text{ mN/m}\}$ is smaller than $\{\omega_D = 10 \text{ rad/s}, E_0 = 2 \text{ mN/m}\}$, which is smaller than $\{\omega_D = 16 \text{ rad/s}, E_0 = 1 \text{ mN/m}\}$).

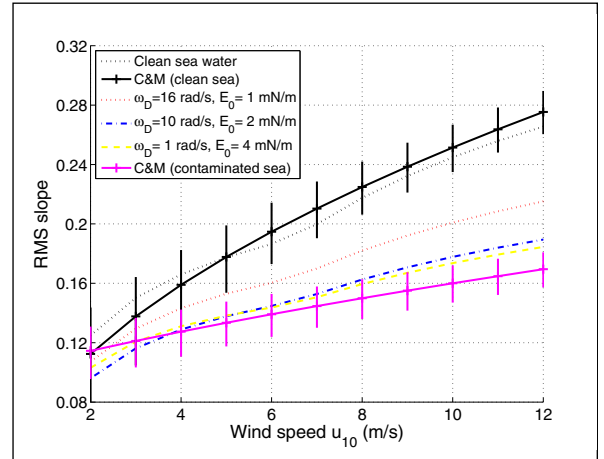


Figure 3. Surface RMS slope of 1-D clean and contaminated sea surfaces versus the wind speed u_{10} . A comparison is also made with the Cox and Munk experimental model.

As explained in [9], with the knowledge of the surface slope spectrum $k^2 S$ of a clean and contaminated 1-D seas, the surface RMS slope can be obtained. Fig. 3 represents the surface RMS slope of 1-D clean and contaminated sea surfaces,

versus the wind speed u_{10} , in the range [2; 12] m/s. It can be seen that the RMS slope of the contaminated (air/oil and oil/sea) interfaces is significantly lower than that of the clean air/sea interface. Moreover, comparatively to the Cox and Munk experimental model, the Lombardini et al. model is slightly higher, for the higher wind speeds u_{10} . This difference can be explained physically. First, the chosen parameters of the Lombardini et al. model were taken to best match experimental results for oil films in Fig. 4 of [15] and Fig. 3 of [14]. Second, the Cox and Munk experimental results were led for a film which cannot strictly be considered as oil. Indeed, it was a mixture consisting of 40 percent used crankcase oil, 40 percent Diesel oil, and 20 percent fish oil. As a consequence, the comparison with the Cox and Munk experimental results is mainly qualitative. It highlights good qualitative agreement with the simulation results of the Lombardini et al. model, the two last configurations giving the best quantitative agreement. As a consequence, the second configuration, $\omega_D = 10$ rad/s and $E_0 = 2$ mN/m, should be a rather typical configuration of oil films and will be retained for numerical simulations of the electromagnetic modeling to follow. Indeed, it is a good compromise between results in Fig. 4 of [15] and Fig. 3 of [14] and the Cox and Munk experimental model.

IV. ELECTROMAGNETIC MODELING: IMPACT ON THE NORMALIZED RADAR CROSS SECTION

Let us have a look at the modification of the normalized radar cross section (NRCS) from the contaminated sea, in comparison with the NRCS of a clean sea surface. From a hydrodynamic point of view, as explained in section II, the clean sea surface (i.e. the air/sea interface) is modeled by the Elfouhaily et al. spectrum model [4], and the contaminated sea (i.e. the air/oil and oil/sea interfaces, where the two interfaces are assumed to be strictly identical and parallel) by the Elfouhaily et al. spectrum model together with Lombardini et al. damping model [5]. To resolve the electromagnetic problem, the benchmark numerical method used here is the Propagation-Inside-Layer Expansion method (PILE) [10], combined to the Forward-Backward method (FB) [11] with Spectral Acceleration (SA) [12], and denoted PILE+FB+SA [13]. This numerical method makes it possible to validate the following semi-empirical approach.

For the case of homogeneous oil slicks covering sea surfaces, the two surfaces are considered as *locally* smooth (flat) (see Fig. 5 of [9]). Then, from the knowledge of the scattering coefficient σ^{oil} of the air-oil interface of the contaminated sea, the scattering coefficient σ^{cont} of the contaminated sea is obtained by multiplying σ^{oil} with the square modulus of the ratio of the equivalent Fresnel reflection coefficient, r_{eq} , of the global system air-oil-sea to the Fresnel reflection coefficient of the air-oil interface, r_{12} :

$$\sigma^{cont} = \left| \frac{r_{eq}(\chi_i)}{r_{12}(\chi_i)} \right|^2 \times \sigma^{oil} \quad (1)$$

with χ_i the local incidence angle. This approximation is consistent with the use of the Kirchhoff approximation (KA), as under this approximation, the considered surfaces are locally

smooth (flat). Then, the local incidence angle $\chi_i \equiv \chi_i^0$ is given by the relation

$$\chi_i = -\frac{(\theta_r - \theta_i)}{2} \quad (2)$$

with θ_i the incidence angle, and θ_r the observation angle. The positive sense is clockwise, then, θ_i being directed counterclockwise, it is negative; θ_r is directed clockwise in the specular direction. This semi-empirical approach, applied to the KA and reduced to the geometric optics approximation (KA+GOA) in the calculation of the NRCS, gives results in good agreement with the reference method around the specular direction (see Fig. 7 of [9] which allowed us to validate this approach when used with the KA+GOA). This result is also in agreement with more qualitative previous works [17,18].

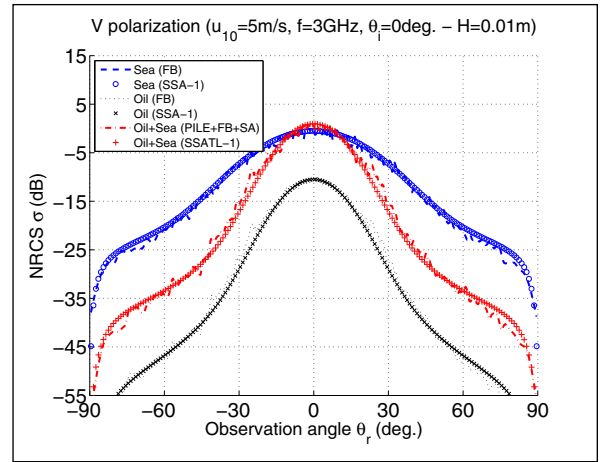


Figure 4. Bistatic scattering coefficients of clean and contaminated seas for V = 10 mm: comparison between the reference numerical method and the SSA-1. The wind speed is $u_{10} = 5$ m/s, the radar frequency $f = 3$ GHz, and the incidence angle $\theta_i = 0$ degrees.

Afterwards, the approach was extended to an asymptotic method which is more adapted to sea surfaces. Fig. 4 represents the semi-empirical approach (denoted as TL for Thin Layer) applied to the first-order of the small slope approximation (SSA-1), denoted as SSATL-1. The wind speed is $u_{10} = 5$ m/s, the radar frequency $f = 3$ GHz, and the incidence angle $\theta_i = 0$ degrees. The parameters of the oil film are $\{\omega_D = 10$ rad/s, $E_0 = 2$ mN/m $\}$, with a film thickness $H = 10$ mm. One can observe a very good agreement of the SSATL-1 with the reference method, at least for observation angles ranging $[-40; +60]$ degrees. Thus, this semi-empirical approach, applied to an appropriate asymptotic model, gives good results for low incidence angles and moderate scattering angles. Moreover, it allows one to obtain the scattering coefficient fast.

In what follows, further investigations are led, in order to test the validity of this semi-empirical approach. For a more precise comparison, the asymptotic models are computed numerically, for a Monte-Carlo process. This has the advantage of comparing the same surfaces. Asymptotic results are obtained from the Kirchhoff Approximation and by using the method of stationary phase (KA+MSP), the first-order small-

slope approximation (SSA1), and the Weighted Curvature Approximation (WCA) [3].

V. NUMERICAL RESULTS: FURTHER INVESTIGATIONS

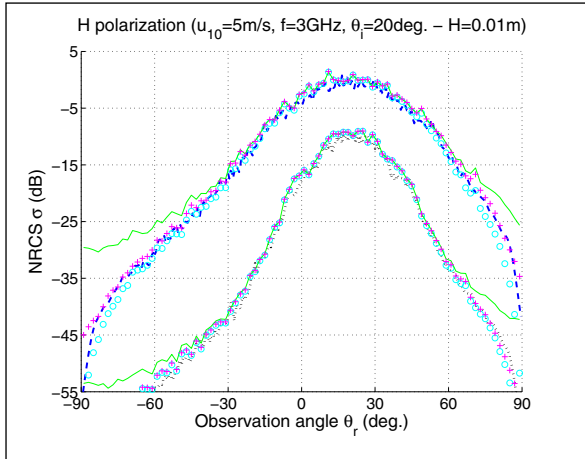


Figure 5. Bistatic NRCS of a clean sea and of the air/oil interface of a contaminated sea for $H = 10$ mm: comparison between the reference numerical method and the KA+MSP, the SSA-1, and the WCA for H polarization.

Fig. 5 presents the numerical results of a clean sea, and of the air/oil interface of the contaminated sea with an oil thickness $H = 10$ mm, for H polarization. The wind speed at 10 m above the sea surface is $u_{10} = 5$ m/s, the radar frequency $f = 3$ GHz, and the incidence angle $\theta_i = 20$ deg. A comparison is made between the reference PILE+FB+SA method, and three models computed numerically. Namely, the KA+MSP without shadowing effect (plotted in full green line), the SSA1 (plotted with cyan circles), and the WCA (plotted with magenta plus signs). The reference PILE+FB+SA method is plotted in blue dashed line for the clean sea and in black dotted line for the air/oil interface.

For V polarization, the numerical results (not presented here) highlight a very good agreement of the asymptotic models with the reference method. Only low differences appear for the SSA1, which underestimates the normalized radar cross section (NRCS) for the clean sea. As well, low differences appear for the KA+MSP for very grazing observation angles θ_r , owing to the fact that it does not take the shadowing effect into account. For H polarization, the same general observations can be done, except from the KA+MSP. Indeed, it overestimates the NRCS for both the clean sea and the air/oil interface, so that it is valid only for θ_r ranging $[-40; +70]$ deg, where good agreement is found though. Other simulations led to the same conclusions. Thus, for the single interface case, for V polarization the three models are in good agreement with the reference method, the best one being the WCA. For H polarization, the same conclusion can be drawn, except from the KA+MSP which is valid only for moderate observation angles θ_r .

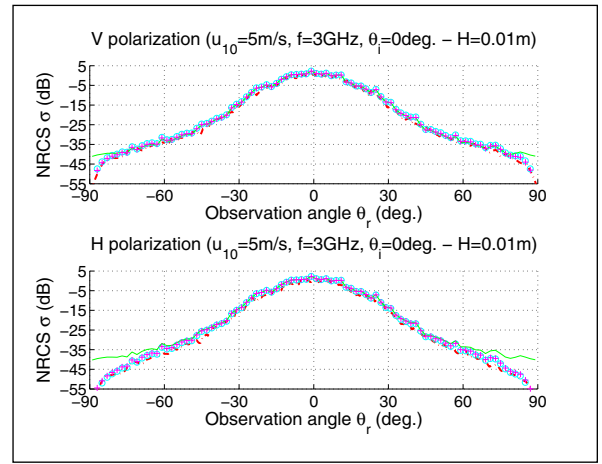


Figure 6. Bistatic NRCS of a contaminated sea for $H = 10$ mm: comparison between the reference numerical method and the KA+MSP, the SSA-1, and the WCA for both V and H polarizations, with incidence angle $\theta_i = 0$ deg.

Fig. 6 presents the numerical results of a contaminated sea for an oil thickness $H = 10$ mm, for both V and H polarizations. The simulation parameters are the same as in Fig. 5, except from the incidence angle $\theta_i = 0$ deg. The reference PILE+FB+SA method is plotted in red dash-dot line. The other models are computed from the calculation of the NRCS of the air/oil interface σ^{oil} , by using equation (1) describing the semi-empirical approach. This figure can be compared with Figs. 9 and 10 of [9], where the semi-empirical approach was applied to the SSA1 computed analytically. Results from Fig. 6, where asymptotic models using the semi-empirical approach are computed numerically, confirm that there is a very good agreement with the reference numerical method. The low differences that appear are very similar to the ones for the single interface case, which confirms the validity of this semi-empirical approach. Other simulations for thinner layers led to the same conclusion, which is not surprising: semi-empirical approach is valid for thin layers, and is getting more precise when the layer thickness decreases. Similarly, numerical simulations for other incidence angles and wind speed lead to the same conclusion and allow to confirm the validation of the thin-layer approach.

Thus, this semi-empirical approach, applied to appropriate asymptotic models like the KA+MSP, the SSA, and the WCA, makes it possible to quantify the scattering from an oil film over the sea surface. This new approach gives results in general very good agreement with the reference method, and makes it possible to obtain numerical results very fast.

REFERENCES

- [1] M.Y. Ayari, A. Coatanhay, and A. Khenchaf, "The influence of ripple damping on electromagnetic bistatic scattering by sea surface," 2005 International Geoscience and Remote Sensing Symposium, Seoul, South Korea, July 2005.
- [2] I.M. Fuks and V.U. Zavorotny, "Polarization dependence of radar contrast for sea surface oil slicks," IEEE Radar Conference, 2007.
- [3] T.M. Elfouhaily and C.-A. Guérin, "A critical survey of approximate scattering wave theories from random rough surfaces," Waves in Random Media, vol. 14, no. 4, pp. R1-R40, 2004.

- [4] T. Elfouhaily, B. Chapron, K. Katsaros, and D. Vandemark, "A unified directional spectrum for long and short wind-driven waves," *Journal of Geophysical Research*, vol. 102, no. C7, pp. 781–96, 1997.
- [5] P.P. Lombardini, B. Fiscella, P. Trivero, C. Cappa, and W.D. Garrett, "Modulation of the spectra of short gravity waves by sea surface films: slick detection and characterization with a microwave probe," *Journal of Atmospheric and Oceanic Technology*, vol. 6, no. 6, pp. 882–90, Dec. 1989.
- [6] W. Alpers and H. Huhnerfuss, "The damping of ocean waves by surface films: a new look at an old problem," *Journal of Geophysical Research*, vol. 94, no. C5, pp. 6251–6265, 1989.
- [7] M. Gade, W. Alpers, H. Huhnerfuss, V.R. Wismann, and A. Lange, "On the reduction of the radar backscatter by oceanic surface films: Scatterometer measurements and their theoretical interpretation," *Remote Sensing of Environment*, vol. 70, no. 66, pp. 52–70, 1998.
- [8] M.Y. Ayari, A. Khenchaf, and A. Coatanhay, "Marine oil-spills electromagnetic scattering model using two-scale model," in *European Conference on Propagation and Systems*, Brest, France, Mar. 2005.
- [9] N. Pinel, N. Déchamps, and C. Bourlier, "Modeling of the bistatic electromagnetic scattering from sea surfaces covered in oil for microwave applications," *IEEE Transactions on Geoscience and Remote Sensing*, vol. 46, no. 2, pp. 385–392, Feb. 2008.
- [10] N. Déchamps, N. de Beaucoudrey, C. Bourlier, and S. Toutain, "Fast numerical method for electromagnetic scattering by rough layered interfaces: Propagation-inside-layer expansion method," *Journal of the Optical Society of America A*, vol. 23, no. 2, pp. 359–69, Feb. 2006.
- [11] A. Iodice, "Forward-Backward method for scattering from dielectric rough surfaces," *IEEE Transactions on Antennas and Propagation*, vol. 50, no. 7, pp. 901–911, 2002.
- [12] H.-T. Chou and J.T. Johnson, "A novel acceleration algorithm for the computation of scattering from rough surfaces with the Forward-Backward method," *Radio Science*, vol. 33, pp. 1277–1287, 1998.
- [13] N. Déchamps and C. Bourlier, "Electromagnetic scattering from a rough layer: Propagation-inside-layer expansion method combined to the forward-backward novel spectral acceleration," *IEEE Transactions on Antennas and Propagation*, vol. 55, no. 12, pp. 3576–3586, Dec. 2007.
- [14] S.A. Ermakov, "Possibilities of identification of oil films using radar probing of the sea surface", 2008 IEEE/OES US/EU-Baltic International Symposium (BALTIC), Tallinn, Estonia, May 2008.
- [15] I. Sergievskaya and S.A. Ermakov, "On wave damping due to oil films", 2008 IEEE/OES US/EU-Baltic International Symposium (BALTIC), Tallinn, Estonia, May 2008.
- [16] C. Cox and W. Munk, "Measurement of the roughness of the sea surface from photographs of the sun's glitter", *Journal of the Optical Society of America*, vol. 44, pp. 838–850, 1954.
- [17] G. Franceschetti, A. Iodice, D. Riccio, G. Ruello, and R. Siviero, "SAR raw signal simulation of oil slicks in ocean environments", *IEEE Transactions on Geoscience and Remote Sensing*, vol. 40, pp. 1935–49, 2002.
- [18] M. Migliaccio, M. Tranfaglia, S. Ermakov, "A physical approach for the observation of oil spills in SAR images", *IEEE Journal of Oceanic Engineering*, vol. 30, pp. 28–39, 2005.